FULL TITLE
ASP Conference Series, Vol. **VOLUME**, **YEAR OF PUBLICATION**
NAMES OF EDITORS

An Automated Ambiguity-Resolution Code for Hinode/SP Vector Magnetic Field Data

K. D. Leka and Graham Barnes and Ashley Crouch

NWRA, CoRA division, 3380 Mitchell Ln., Boulder, CO 80301 USA

Abstract. A fast, automated algorithm is presented for use in resolving the 180° ambiguity in vector magnetic field data, including those data from Hinode/Spectropolarimeter. The Fortran-based code is loosely based on the Minimum Energy Algorithm, and is distributed to provide ambiguity-resolved data for the general user community. Here we generally describe the released code (available at `www.cora.nwra.com/AMBIG`), examples of its performance and usage for Hinode/SP data.

Automated Ambiguity Resolution

Vector magnetic field observations which utilize both the circular and linear state of polarization of magnetically-sensitive spectral lines suffer from an inherent limitation. Due to a degeneracy at the atomic level, the direction of the magnetic field transverse to the line of sight is ambiguous to 180°. After the inversion from spectropolarimetric signal to field strength and relevant angles, some method must be employed in order to resolve this ambiguity and determine the true solar magnetic vector, in order to utilize the "magnetogram" in a physically meaningful way.

Numerous algorithms have been developed for this problem with a variety of assumptions and implementations. Recently, efforts have been made to quantitatively evaluate their performances when tested against simulations of observational challenges (Metcalf et al. 2006; Leka et al. 2009). The NCAR/HAO "`AZAM`" utility has been widely used for data from the Hinode/SpectroPolarimeter (Tsuneta et al. 2008; Ichimoto et al. 2008), and it is generally very high-scoring for the tests mentioned above. However, as an interactive approach `AZAM` is challenging to employ objectively for all available data. We present an automated approach which will allow researchers to physically interpret the magnetic state of the solar atmosphere without being expert in inversion or ambiguity-resolution science.

The Underlying "Minimum Energy" Algorithm

The code seeks an optimal solution based on physically defensible arguments about the state of the Solar atmosphere. The Minimum Energy algorithm (Metcalf 1994) globally minimizes a functional containing approximations to both the electric current density, J, and the field divergence. Minimizing $\nabla \cdot \mathbf{B}$ gives a physically meaningful solution and minimizing J provides a smoothness constraint.

Since the calculation of J and $\nabla \cdot \mathbf{B}$ involve horizontal derivatives of the magnetic field, the computation is not local. A global optimization is required; a

"simulated annealing" algorithm (Metropolis et al. 1953; Kirkpatrick et al. 1983) is used to minimize the functional, an approach that is appropriate for a problem based on discrete solutions (two and only two possibilities at each pixel) that also presents many local minima.

The calculation of the vertical electric current density, J_z, is straightforward, requiring only observed quantities in the computation and a choice of the ambiguity resolution. However, calculation of $\nabla \cdot \mathbf{B}$ and the horizontal components of the current requires knowledge of the vertical derivatives of the magnetic field which are typically obtained from a force-free extrapolation.

The ME algorithm (Metcalf 1994) evolved substantially since its inception. Photospheric vector magnetograms rarely present a boundary consistent with a linear force-free field, so eventually a variety of optional functionals, weighting options, and different optimization schemes were included (Metcalf et al. 2006). Coded in the Interactive Data Language (IDL), ME was criticized for being too slow and user-intensive, essentially defeating its original purpose.

Present Implementation

What is presented here is loosely based on the original ME algorithm. The basic approach remains: simulated annealing is used to globally minimize the functional $\sum(|J_z| + |\nabla \cdot \mathbf{B}|)$. Input can be as formatted arrays or FITS files, specified as $[|B|, \gamma, \phi]$ or $[B_\parallel, B_\perp, \phi]$; it is assumed that the magnetic fill factor has been propagated through, so that the field components are in units Mx/cm^2.

In this released version, the essence of the algorithm is retained while making it usable for routine implementation:

- For simplicity, $\partial B_z/\partial z$ is approximated from a potential field extrapolation using the unambiguous line-of-sight field as the lower boundary condition. While this represents a "step back" from the direction ME was moving, tests show that when used in the context of a global optimization, derivatives based on a potential field are sufficient.

- To prevent ringing in the FFT-based approach for calculating the derivatives, the line-of-sight boundary field is extended with a buffer field, and a bi-cubic spline applied between the original field and the buffer to ensure a smooth transition between the two.

- The functional to be minimized relies on J_z rather than an approximation of the vector $\mathbf{J}$ which reduces the needed computations and removes reliance on derivatives needed for J_x, J_y.

- Pixels with $B_\perp$ magnitudes deemed to be below an appropriate noise level are solved using a nearest-neighbor acute-angle approach, propagating the "correct" solution resulting from the global minimization to areas dominated by noise.

- The full code is written in Fortran using FITSIO for flexible data handling and FFTW for optimal computation of the potential-field derivatives.

Various input parameters can be set when the code is run, such as cooling schedules (slower cooling can better avoid sub-optimal results) and factors related to mitigating FFT-caused ringing. The magnitude of the transverse

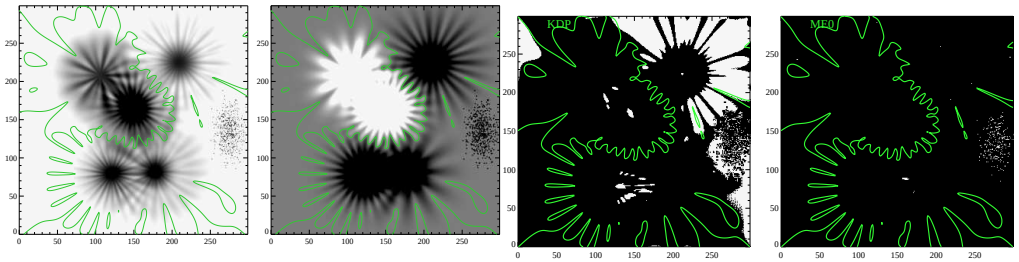

Figure 1. (**Left to Right:**) "Continuum Intensity" and vertical field from an analytic model constructed to test the effects of unresolved fine-scale structure, with the magnetic neutral line also shown for reference; the results of a potential-field acute-angle solution and the automated ME-based solution: black/white are where solutions are/are not correct, with the same neutral-line plotted for reference. See (Leka et al. 2009) for details.

component of the field below which the nearest-neighbor acute-angle smoothing is invoked (the "below-threshold" value), is a parameter which can be set. For our testing with both analytic and Hinode/SP data, an appropriate level for the acute-angle smoothing was found to be in the range $200 \lesssim B_\perp \lesssim 400$ Mx/cm^2.

Performance

Tests were performed to challenge the presented code against off-disk-center observations, photon noise, non-constant-α boundaries, and the effects of imperfect spatial resolution (Metcalf et al. 2006; Leka et al. 2009). Model data were used and performance judged objectively since the answer was known. As an example, to test the effects of spatial resolution, a model field was constructed to mimic $0''.3$ Hinode/SP observations of fine-scale (unresolved) solar structure. An example of the performance of this automated algorithm against a potential-field acute-angle method for this case is shown in Figure 1; many objective metrics were used to evaluate the performance of this and other methods (see Table 1), and it performed as well as or better than all other algorithms submitted, including the latest and most option-filled version of the IDL-based minimum-energy

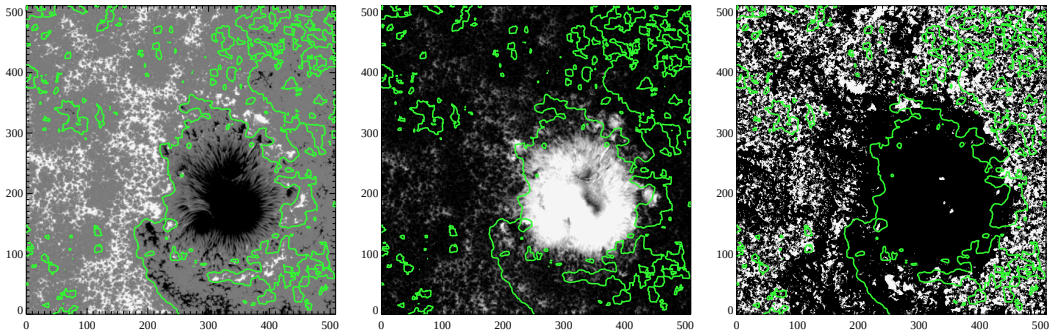

Figure 2. **Left:** Vertical Field B_z of NOAA AR 10953 observed 30 April 2007 by the Hinode/SOT SpectroPolarimeter; white/black areas denote positive/negative area-averaged field scaled to $\pm$1000Mx/cm^2, green is a smoothed magnetic neutral line. **Middle:** Same but for $B_\perp$, scaled $0 \lesssim B_\perp \lesssim$ 1000Mx/cm^2. **Right:** Comparison of the azimuthal ambiguity resolution between the auto-ME and `AZAM`; black/white indicates where the algorithms do/do not agree, with the smoothed magnetic neutral line for reference.

Table 1. Performance Metrics

Metric:	$\mathcal{M}_{\rm area}$	$\mathcal{M}_{\rm Bz}$	$\mathcal{M}_{B_\perp>100{\rm G}}$	$\mathcal{M}_{\rm I}$	$\mathcal{M}_{\Delta\mathbf{B}}$
	$\frac{\#{\rm pix}(\Delta\theta=0)}{\#{\rm pix}}$	$\frac{\sum\lvert B_(\Delta\theta=0)\rvert}{\sum\lvert B_z\rvert}$	$\frac{\sum B_\perp(\Delta\theta=0)}{\sum B_\perp}$	$\sum \mid J_{\rm z} \mid$	$\frac{\sum\lvert\mathbf{B}(s)-\mathbf{B}(a)\rvert}{\#{\rm pix}}$
Units:				1^{13}Amp	Mx/cm^2
Best is:	1.0	1.0	1.0	low	0.0
Test-Cases in Figure 1, answer *vs.* **known solution:**					
Potential:	0.83	0.92	0.94	2.0	74
Auto ME:	1.0	0.98	1.0	0.48	0.8
Hinode/SP example, Figure 2, AZAM *vs.* **Auto-ME:**					
	0.72	0.88	0.97	18(A) 16(ME)	22

code and `AZAM`. As the metrics show, methods generally agreed in strong-$B_\perp$ areas but even when they do, there can be a significant difference between the amount of additional noise that is effectively added by the ambiguity resolution (the $\mathcal{M}_{\Delta\mathbf{B}}$ metric).

On a modern PC, a 512^2 pixel Hinode/SP magnetogram takes roughly ten minutes to complete, with variations allowed for processor speed, cooling schedule, and the below-threshold value.

Example from Hinode/SP

For all remotely-sensed observational magnetic field data, there is no certainty as to what constitutes the correct answer. We show here a comparison between the automated solution and `AZAM` both graphically in Figure 2, and using metrics computed for the two in Table 1 (rather than compared to a known answer, as above).

Both modes of comparison show that the two methods agree in areas of strong transverse field; the global minimization of a functional which includes J_z indeed results in a lower total vertical current as compared to `AZAM`. The areas near a recently-studied emerging filament (Okamoto et al. 2008) agree to a large extent, solidifying the interpretation presented in that study as not being susceptible to uncertainties in the ambiguity resolution outcome.

Acknowledgments. We are grateful to Dr. Bruce Lites for providing Hinode/SP data and the results of the AZAM disambiguation. KDL, GB and AC acknowledge funding from NASA/LWS under contract NNH05CC75C and the NWRA subcontract from SAO under NASA NNM07AB07C. The ME0 code was in part tested and developed with funding to NWRA through the HMI project at Stanford University, NASA NAS5-02139.

References

Ichimoto, K. et al. 2008 Solar Phys.249, 233.
Kirkpatrick, S., Gelatt, C.D., Vecchi, M.P. 1983, *Science* 220, 671
Leka, K. D. et al 2009, Solar Phys., in submission.
Metcalf, T. R. 1994, Solar Phys., 155, 235
Metcalf, T. R. et al 2006, Solar Phys., 237, 267
Metropolis, N., Rosenbluth, A., Rosenbluth, M., Teller, A., Teller E. 1953, J. Chem. Phys. 21, 1087
Okamoto, T. J. et al 2008, ApJ673, L215
Tsuneta, S. et al. 2008 Solar Phys.249, 167